analytical chemistry

pubs.acs.org/ac Article

Epidermal Patch with Glucose Biosensor: pH and Temperature Correction toward More Accurate Sweat Analysis during Sport Practice

Alexander Wiorek,[†] Marc Parrilla,[†] María Cuartero, and Gastón A. Crespo*

Cite This: *Anal. Chem.* 2020, 92, 10153−10161 Read Online

ACCESS | Metrics & More | Article Recommendations | Supporting Information

ABSTRACT: We present an epidermal patch for glucose analysis in sweat incorporating for the first time pH and temperature correction according to local dynamic fluctuations in sweat during on-body tests. This sort of correction is indeed the main novelty of the paper, being crucial toward reliable measurements in every sensor based on an enzymatic element whose activity strongly depends on pH and temperature. The results herein reported for corrected glucose detection during on-body measurements are supported by a two-step validation protocol: with the biosensor operating off- and on-bodily, correlating the results with UV−vis spectrometry and/or ion chromatography. Importantly, the wearable device is a flexible skin patch that comprises a microfluidic cell designed with a sweat collection zone coupled to a fluidic channel in where the needed electrodes are placed: glucose biosensor, pH potentiometric electrode and a temperature sensor. The glucose biosensor presents a linear range of response within the expected physiological levels of glucose in sweat (10−200 μM), and the calibration parameters are dynamically adjusted to any change in pH and temperature during the sport practice by means of a new "correction approach". In addition, the sensor displays a fast response time, appropriate selectivity, and excellent reversibility. A total of 9 validated on-body tests are presented: the outcomes revealed a great potential of the wearable glucose sensor toward the provision of reliable physiological data linked to individuals during sport activity. In particular, the developed "correction approach" is expected to impact into the next generation of wearable devices that digitalize physiological activities through chemical information in a trustable manner for both sport and healthcare applications.

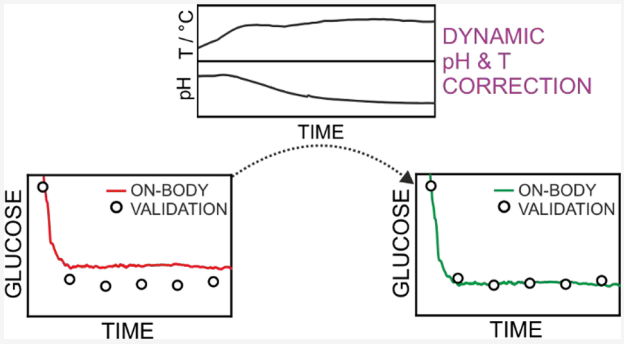

Epidermal wearable chemical sensing technology allows for the continuous profiling of distinct biomarkers (i.e., ions and molecules) in sweat during perspiration, and this is highly significant to understand the physiology of individuals under certain activities and ultimately to provide a personalized training routine.[1] Noteworthy, wearable sensor patches are not only restricted to sport-physiology, and in fact, the science behind its development envisions to promote the true digital transformation of the body-status in the broadest sense:[2−4] this includes clinical diagnosis supported by artificial intelligence to shed light on prediction patterns.

Most of the papers about epidermal sensing patches focuses the discussion and purpose of the investigation on sport-physiology, but rarely, strict validations using a gold-reference and pilot tests are depicted. This may likely be one of the reasons to understand the lack of these devices in the commercializing pipeline for sweat sensing, whereas the interest of general people and market is undoubtedly high.[5] In this regard, we have recently reported on a rather detailed guideline for sweat sampling based on the regional absorbent patch method, aiming at the suppression of potential bias in the final correlation of on-body data once the wearable patch is cross-validated based on sweat sampling.[6]

Importantly, epidermal wearable ion-sensing has been exhaustively covered by the Javey group with elegant descriptions of the circuitry, stretchable materials, apps and spiral-patterned microfluidic channel, among others.[7−9] Recently, our group has gone one step forward in terms of simplicity in microfluidic integration, cytotoxicity, strictness of the analytical validation, representative number of on-body tests, and as worth mentioning, the verification of genuine and accurate chemical information.[6,10] Apart from ions (i.e., electrolytes), there are other relevant biomolecules that captivate the attention of physiologist and clinician from the body-status point of view such as glucose, lactate, and

Received: May 23, 2020
Accepted: June 12, 2020
Published: June 26, 2020

https://dx.doi.org/10.1021/acs.analchem.0c02211
Anal. Chem. 2020, 92, 10153−10161

ethanol.[11,12] In particular, while the importance of glucose sensing is well-known in terms of diabetes monitoring and therapy, there are a number of open questions about physiological relevance in sport, the correlation between blood/sweat in such aerobic/anaerobic conditions, and, finally, the partition mechanism from blood to sweat. This is the reason for new glucose (bio)sensors arising daily in the literature.[13]

The group of Kim has been working on graphene-based electrochemical devices for glucose sensing in sweat.[14] Although, the stretchable device is rather focused on diabetes therapy (i.e., it delivers a drug from loaded-microneedles once the level of glucose is high [hyperglycemia]), there are some insightful aspects related to the analytical performance of the glucose sensor. Indeed, Kim et al. suggested the necessity of pH and temperature (T) correction for enzyme-based sensors, an important point seldom mentioned in glucose wearable sensor assessments.[14] Perspiration is a dynamic process that involves fluctuations in pH and T during sport practice, being also levels and trends completely different comparing several subjects (approximately 2 units in pH and a range of ca. 20−40 °C for the T). These fluctuations are expected to influence the biosensor response as a result of changes in the activity of the enzyme on which the sensor is based.[15] This puts in evidence the necessity to evaluate those effects off-site, off-body, and on-body to achieve an accurate monitoring of glucose. In this sense, Javey and co-workers reported on T compensation[4] while Kim et al. reported on both T and pH correction of the glucose profile for short analysis time (less than 10 min).[14]

In this rich and exciting context about epidermal sweat sensing progress, in particular for glucose detection, we understand that there is a lack of a systematic study proving the importance of pH and T correction while sweat is flowing through a microfluidic cell for an extensive period of time (1 h), which is representative of sport training. In contrast to the current state of the art, we feel the necessity to ensure the quality (i.e., accuracy) of the provided data by using the sampling method published recently by our group.[6] Overall, we propose herein an analytical protocol to correct the data provided by the glucose epidermal patch based on pH and T measurements in sweat (i.e., inside the microfluidic cell) as well as a validation based on sweat collection. Indeed, we have developed a novel sensing and fluidics design for glucose, pH, and T monitoring in sweat and use it as proof-of-concept during cycling. Finally, the validated on-body data fully demonstrates the relevance of the epidermal patch with the glucose biosensor to monitor a continuous profile in sweat of different subjects during physical activity in a total of 9 on-body tests at different conditions (T1−9).

EXPERIMENTAL SECTION

Fabrication of the Sensor Array. Figure 1a−c illustrates the glucose, pH, and T sensors fabricated on a flexible polyester sheet (0.125 mm thick, RS components, Sweden) as the substrate. The glucose sensor consists of a three-electrode system, each of them prepared on individual circular patterns (2 mm of diameter and separated in 2 mm between them) that were connected to a straight path (8 mm long) that is screen-printed using Ag/AgCl ink (C2131007D3, Gwent group, U.K.) and serving for further electrical connections. The circular patterns for the working and counter electrodes (WE_1 and CE) were prepared with carbon ink (C2030519P4, Gwent group, U.K.), while the reference electrode (RE_1) consisted of just the straight track made of Ag/AgCl. Subsequently, the WE_1 surface was modified with Prussian blue mediator (PB), an enzymatic layer (i.e., chitosan and glucose oxidase, CHI + GOx), and external polymeric layer (i.e., Nafion). The pH sensor was fabricated using the same conductive pattern as for the glucose biosensor, this time being composed of a working electrode (WE_2) and a reference electrode (RE_2) for the potentiometric readout. Subsequently, the WE_2 and RE_2 were modified first with a layer of multiwalled carbon nanotubes (MWCNTs) and thereafter with the pH selective membrane (pHSM) and the reference membrane (RM) on top, respectively (see the Supporting Information for the membrane compositions). For the T sensor, two electrodes based on straight Ag/AgCl ink were used. These electrodes were electrically connected by drop casting MWCNTs dispersed in THF. For further details on the manufacturing of each electrode, the reader is referred to the Supporting Information.

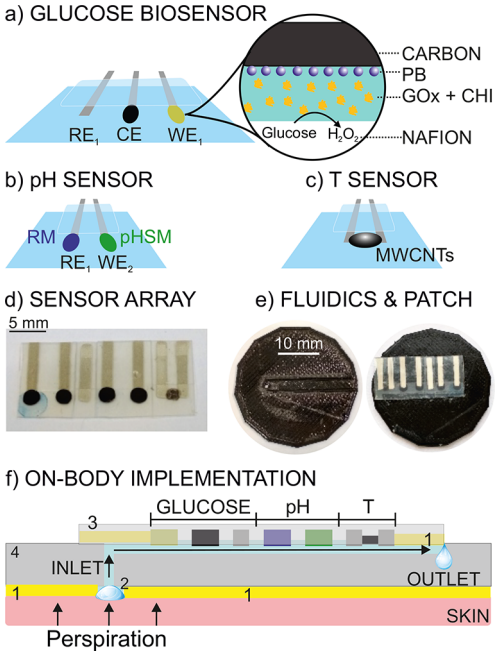

Figure 1. (a) Glucose biosensor. In yellow, the WE_1 modified with the PB, the enzyme-based layer (GOx + CHI) and Nafion. In black, the carbon-based CE. The RE_1 is an Ag/AgCl rectangular path. The electrode patterns are protected by a layer of adhesive tape. (b) pH potentiometric sensor. In green, the WE_2 modified with the pH selective membrane (pHSM). In blue, the RE_2 modified with the reference membrane (RM). (c) Temperature sensor comprising two Ag/AgCl electrodes connected by a layer of MWCNTs. (d) Image of the sensor array. (e) Images of the microfluidic cell (containing a hole as the collection zone and the microfluidic channel) and the skin patch (the electrodes are placed in the microfluidic channel). (f) Illustration of the patch attached to the skin. Arrows indicate the sweat flow direction. 1: Adhesive transfer tape. 2: Sweat collection zone. 3: Sensor platform. 4: Microfluidic cell.

Implementation of the Sensors into the Microfluidic Cell for On-Body Measurements. The sensor array (Figure 1d) was then attached to a 3D-printed microfluidic cell (Figure 1e) by using adhesive transfer tape (3 M 9471LE), so that the electrodes were placed coinciding with the microfluidic channel (see the Supporting Information for specific details). For on-body measurements, the device was attached to the individual skin on the forehead by adhesive transfer tape

https://dx.doi.org/10.1021/acs.analchem.0c02211
Anal. Chem. 2020, 92, 10153−10161

(Figure S1 in the Supporting Information), thereby avoiding any possible leaking of sweat and allowing for an adequate pressure from the eccrine glands to provide continued and passive sweat flow during perspiration.[16] A circular collection zone (diameter of 0.1 mm, thickness of 1 mm) was used to sample the sweat, being connected to a fluidic channel where the electrodes are embedded (Figure 1e,f). As the total area of the zone just before the electrodes is 133 mm^2 with an approximate volume of 6.7 μL, the sweat will start flowing through the surface of the first electrode after ca. 5 min of the perspiration starting. The fluidic channel contains an internal volume of approximately 4 μL. Thus, considering the initial time needed to fill in the collection area and a typical perspiration rate of 1 $\mu L\ cm^{-2}\ min^{-1}$ for a midintensity, it will take ca. 10−13 min to display a reliable sweat profile after the sweat reaches the surface of all of the electrodes in the array.

RESULTS AND DISCUSSION

The analytical performance of the glucose biosensor was characterized prior to its implementation in the microfluidic cell. The biosensor presented a linear range of response from 10 to 1500 μM, with a variation coefficient of less than 4% for the calibration parameters (slope and intercept) for six consecutive calibration graphs using the same electrode (Figure S2a,b in the Supporting Information). Acceptable between-electrode reproducibility (n = 6 different electrodes) was found, in all the cases showing the same linear range of response (Figure S3a in the Supporting Information), which is important toward on-body measurements. Furthermore, very low midterm drift was displayed by the biosensor (100 μM glucose solution: 7.7 ± 1.1 nA h^{-1} over 2 h). The response time was calculated to be in the range of 4−7 s, which reflects rather fast response. Excellent reversibility was also obtained, with deviations of less than 5% for the amperometric signal (Figure S2c,d in the Supporting Information). The glucose biosensor did not present any response toward lactate, pyruvate, uric acid, and ascorbic acid at the expected levels in sweat, and therefore, no matrix effect is expected in real sweat measurements (see Figure S3b in the Supporting Information). Because pH and T changes in the sample are expected to influence the performance of any enzymatic biosensor, the evaluation of the glucose biosensor calibration under different pH and T conditions was accomplished (Figure 2). For example, the T in sweat may range from 26 to 38 °C depending on the body region, and pH varies from 4 to 7.5 between subjects.[3,7,17−19] Figure 2a,b show the dynamic response and corresponding calibration curves for the biosensor after changing the pH of the background solution (i.e., standard additions of glucose to either acetate of phosphate buffers of different pH).

There is a clear dependence of the amperometric signal with the pH: the slope decreased and the first glucose concentration that the biosensor was able to detect increased with more acidic pH background; that is, the lower the pH, the more negative the baseline and this creates that lower glucose concentration are not detected by the biosensor. In principle, this is a direct consequence of the reduction of the enzyme activity with the pH.[15]

Figure 2c depicts the dynamic response of the biosensor at increasing T in the sample. As observed, the amperometric signal was enhanced with increasing T, which is in principle expected owing to the increment of the enzymatic activity with T. Furthermore, we confirmed that drastic changes in either

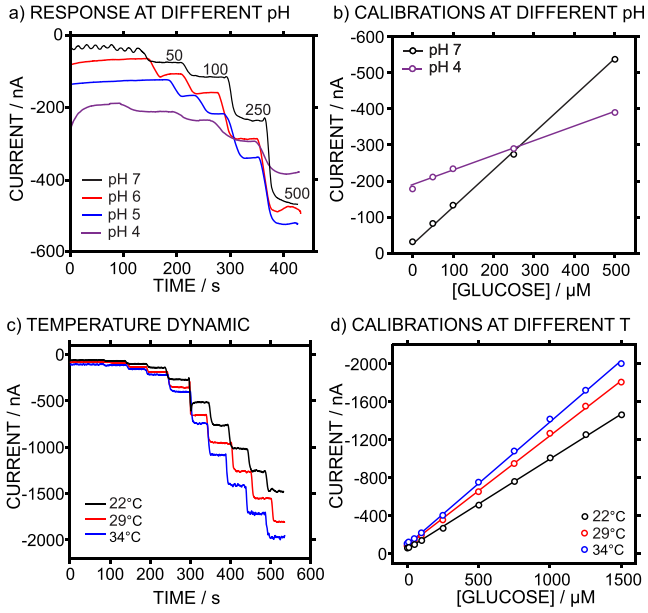

Figure 2. (a) Dynamic response of the biosensor toward increasing glucose concentrations in background of different pH. The final concentration of glucose is indicated in each signal change. All the experiments were accomplished using the same electrode. (b) Calibration graphs corresponding to pH 7 and 4. (c) Dynamic response of the biosensor at increasing glucose concentration in 10 mM phosphate buffer solution (100 mM NaCl) at pH 6.6 and changing the T of the solution. All of the experiments were accomplished using the same electrode. (d) Corresponding calibration graphs. The biosensor was interrogated by applying a constant potential of −0.05 V versus the Ag/AgCl reference electrode and under stirred conditions.

pH or T does not deteriorate the biosensor response and therefore, any current change is reversible. For this purpose, we evaluated the response at a fixed glucose concentration before and after changing the pH from 7 to 4 and T from 22 to 37 °C (Figure S4 in the Supporting Information). Despite the current changing in more than 100 nA for drastic changes in pH and T, the initial response of the biosensor did not deteriorate and was rather reversible, thus recovering the initial current value after drastic changes in pH and T (change in the initial current lower than 1% was observed).

In Vitro Evaluation of the Analytical Performance of the Glucose Biosensor after Implementation in the Microfluidic Cell. To characterize the analytical performance of the glucose biosensor once implemented in the microfluidic cell (i.e., flow mode), a flow rate of 4 $\mu L\ min^{-1}$ (achieved by means of a peristaltic pump) was selected. This flow rate corresponds to a sweat rate of 3 $\mu L\ cm^{-2}\ min^{-1}$, which is close to reported values of 2.4 $\mu L\ cm^{-2}\ min^{-1}$ achieved under mild activity conditions during on-body tests accomplished on the forehead.[20] Figure 3a presents four successive dynamic responses (replicates) at increasing glucose concentrations in artificial sweat background, and Figure 3b shows the corresponding calibration graphs with the error bars displaying the standard deviation for the measurements. The repeatability of the calibration parameters was rather good (less than 3% of variation, slope of 1.14 ± 0.03 nA μM^{-1} and intercept of −50.7 ± 1.1 nA), while keeping the linear range of response within the expected physiological range in sweat: from 10 to 200 μM.[21,22] Other reported glucose biosensors, slightly exceed the

https://dx.doi.org/10.1021/acs.analchem.0c02211
Anal. Chem. 2020, 92, 10153−10161

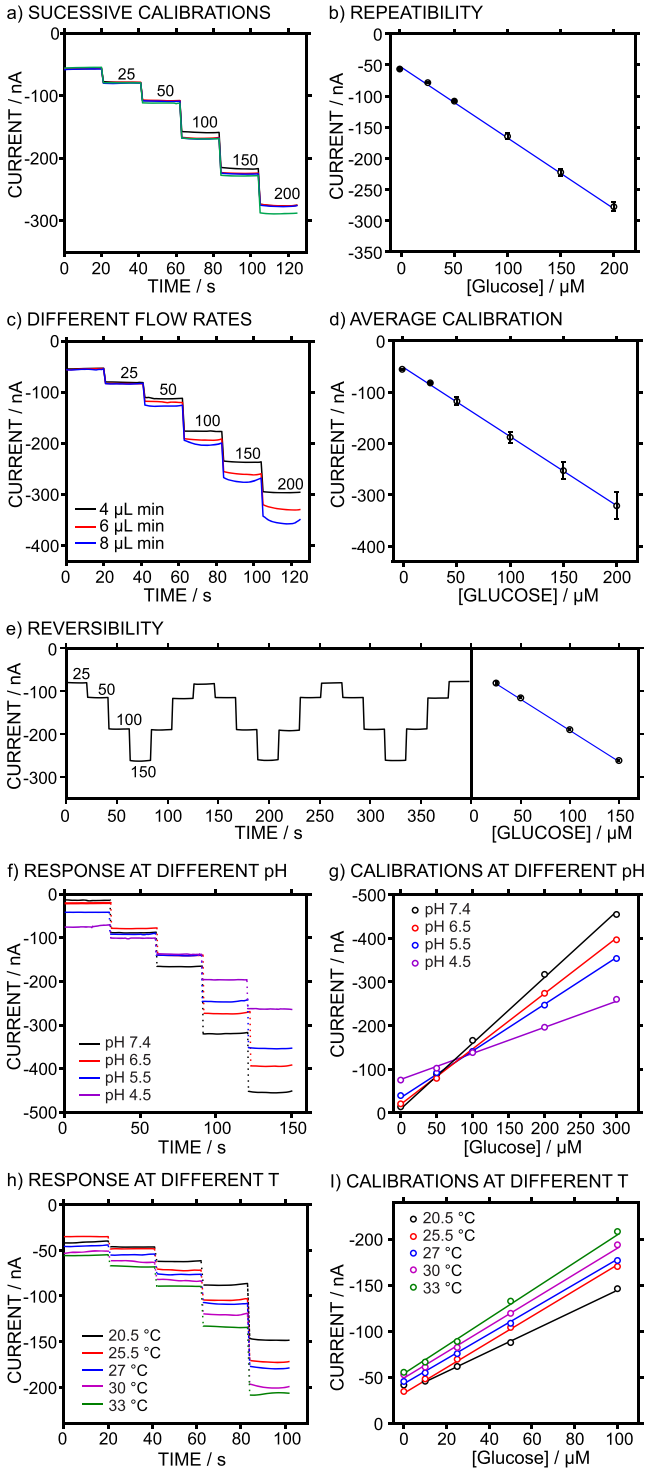

Figure 3. (a) Successive dynamic responses (replicates, $n = 4$) of the glucose biosensor under flow mode (4 μL min^{-1}) in artificial sweat background (pH 6.6). The final concentration of glucose is indicated in each signal change. (b) Average calibration curve with error bars showing the standard deviation (slope of -1.14 ± 0.03 nA μM^{-1} and intercept of -50.7 ± 1.1 nA). (b) Dynamic response of the glucose biosensor at increasing flow rates in artificial sweat background (pH 6.6). (c) Average calibration curve observed at increasing flow rates (slope of -1.36 ± 0.13 nA μM^{-1} and intercept of -49.4 ± 1.0 nA). The final concentration of glucose is indicated in each signal change. (d) Dynamic response and average calibration graph observed in the reversibility test (4 μL min^{-1}) in artificial sweat background (pH 6.6): Slope of -1.45 ± 0.01 nA μM^{-1} and intercept of -43.9 ± 1.8 nA. (e) Dynamic response and average calibration graph observed before and after torsion strain to the microfluidic cell containing the glucose biosensor (4 μL min^{-1}) in artificial sweat background (pH 6.6): Slope of -1.49 ± 0.13 nA μM^{-1} and intercept of -23.2 ± 1.4 nA. The final concentration of glucose is indicated in each signal change. (f) Dynamic responses at decreasing pH. (g) Corresponding calibration graphs. (h) Dynamic response at different T in artificial sweat background (pH 6.6). (i) Corresponding calibration graphs.

lower concentration of this range.[23] The response time of the biosensor in flow mode was lower than 20 s along the linear range of response, considering all the time traces obtained along this work. This is a fast response and indeed very convenient for the acquisition of real time data during on-body tests.

During sport practice (or workout), slight changes in the sweating rate of the subject are expected.[24] Therefore, the response of the biosensor was evaluated at three different flow rates (4, 6, and 8 μL min^{-1}, selected as per mimicking real sweat rates in the body during sport practice[24]). Figure 3c depicts the dynamic responses at the different flow rates, and Figure 3d shows the average calibration graph. As observed, the response of the biosensor increased with the flow rate and this is specially noticed at higher glucose concentrations (from 100 μM). According to the standard deviations observed in the calibration parameters of the average calibration graph (slope of 1.36 ± 0.13 nA μM^{-1} and intercept of -49.4 ± 1.1 nA), it was calculated that, the most drastic change in the sweat rate may induce an error of less than the 10% in the calculation of the glucose concentration, which is an acceptable level in precision considering further physiological measurements.[25] This error will specially affect higher concentrations (>100 μM), which indeed were never observed in any of the on-body tests developed in the present work. The glucose conversion rate at the enzyme layer is connected to the concentration gradient of glucose in the external membrane phase (Nafion), and it is expected that at higher flow rates the glucose concentration gradient is more established and sustained given the faster replenishment of glucose once the aqueous diffusion layer is reduced.

Beyond any change in the flow rate, the between-electrode reproducibility (using different twin electrodes) was found to be rather good, with less than 1.2% of change in the calibration parameters (see Figure S5 in the Supporting Information). Then, a reversibility test was performed by changing the concentration of glucose from 25 to 150 μM and from 150 to 25 μM along three cycles (see Figure 3e). The biosensor exhibited a very reversible response with a change in the calibration parameters of less than 4%: average calibration graph with slope of 1.45 ± 0.01 nA μM^{-1} and intercept of 43.9 $\pm$ 1.7 nA. In addition, the biosensor presented excellent drift in flow mode at 4 μL min^{-1} (1.3 nA h^{-1} over 2.5 h, even lower value than in batch mode). Advantageously, the analytical response of the biosensor is maintained after applying a strong torsion strain. Thus, the calibration graph was found to be maintained in the accomplished resilience test (see Figure S6 in the Supporting Information): less than 5% of change in the calibration parameters.

Similar as in batch mode, the influence of the pH and T in the response under flow conditions was investigated (Figures 3f–i). In both cases, if the pH or the T decreases significantly

https://dx.doi.org/10.1021/acs.analchem.0c02211
Anal. Chem. 2020, 92, 10153−10161

in sweat, the biosensor presents a loss of sensitivity together with a shift of the intercept (or background signal) to more negative currents. Importantly, the trends found for both pH and T influences will be subsequently used to elaborate a correction of the amperometric response of the glucose biosensor.

pH- and Temperature Correction for the Amperometric Response of the Glucose Biosensor. Sensors for monitoring pH and T fluctuations in the sweat analyzed by the glucose biosensor were implemented in the microfluidic cell (i.e., the entire epidermal patch). The details for the handmade fabrication are provided in the Supporting Information. Briefly, the pH sensor consists of a potentiometric one based on a WE_2 and a RE_2 prepared as reported elsewhere[6] but on the same polyester substrate used to fabricate the biosensor. The temperature sensor is based on a chemoresistor principle, where the resistance of carbon nanonotubes linearly depends on the temperature.[26,27]

The pH sensor displayed a reproducible near-Nernstian slope of −53.8 ± 0.1 mV and intercept of 343.5 ± 16.3 mV (Figures 4a and S7a in the Supporting Information, n = 3),

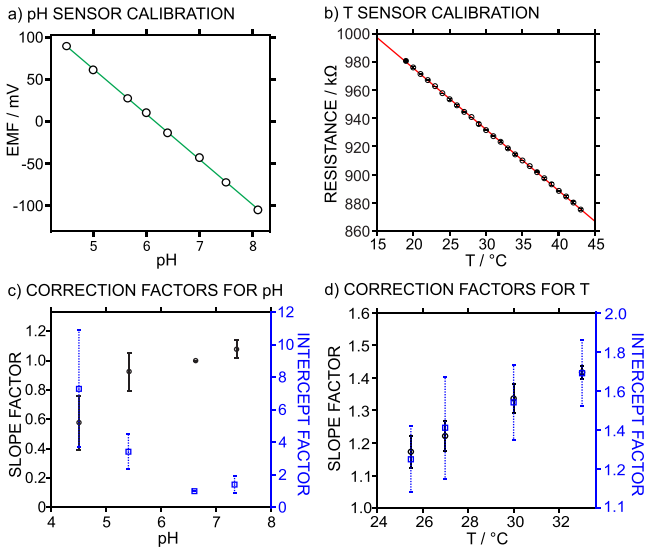

Figure 4. (a) Calibration graph of the pH sensor (T = 20 °C). (b) Calibration graph of the T sensor in artificial sweat background (pH 6.6). (c) Correction factors (f) as a function of sweat pH for the calibration parameters of the glucose biosensor. (d) Correction factors (g) as a function of sweat T for the calibration parameters of the glucose biosensor.

with excellent reversibility of the calibration parameters (slope of −52.9 ± 0.6 mV and intercept of 325.0 ± 4.2 mV, Figure S7b in the Supporting Information) within a linear range of response from pH 4.5 to 8.1, which contains the physiological range expected for pH in sweat (pH 4.5−7.5).[4] Good performance was also observed for the T sensor: slope of −4.4 ± 0.1 kΩ °C^{-1} and intercept of 1063.4 ± 0.2 kΩ for three successive calibrations (Figure 4b), within a linear range from 19 to 43 °C and showing excellent reversibility (less than 3.5% of variation in the calibration parameters, see Figure S8 in the Supporting Information). Both sensors presented neglectable influence of torsion application on the calibration parameters (applying the same resilience test as for the glucose biosensor, see Figure S6 in the Supporting Information, calibration parameters changed <1.2% in both cases).

Next, we elaborate on the pH and T correction of the glucose concentration dynamic assuming that the effects of pH and T on the biosensor (i.e., the enzyme) are independent from each other and that every single glucose biosensor presents the same kind of influence from pH and T variations. Accordingly, it is possible to universally tabulate the individual effect of pH and T in the slope and intercept of every glucose biosensor by calculating a factor of variation (f_{slope} and $f_{intercept}$ for the pH and g_{slope} and $g_{intercept}$ for the T) at each condition with respect to the reference conditions of pH 6.6 and T of 20 °C, using the following equations:

$$f_{slope} = \frac{slope_{pH}}{slope_{6.6}} \quad (1)$$

$$f_{intercept} = \frac{intercept_{pH}}{intercept_{6.6}} \quad (2)$$

$$g_{slope} = \frac{slope_{T}}{slope_{20}} \quad (3)$$

$$g_{intercept} = \frac{intercept_{T}}{intercept_{20}} \quad (4)$$

Figure 4c,d shows the correction factors for the slope and intercept calculated at different pH and T in sweat, from the data collected in Figure 3f−i and using eq 1−4. Notably, the errors bars refer to the measurements of three different electrodes. As observed, the pH has a larger effect than the T on the biosensor response, specifically in the intercept, and this is manifested in higher correction factors.

Considering now pH and T effects in accumulative way, it is possible to correct the entire response of the biosensor on the basis of recalculating the slope and intercept (k and m respectively) of the initial off-body calibration graph in artificial sweat (at pH 6.6 and 20 °C for reference). Thus, by applying a first-order correction algorithm, we dynamically calculate the corrected slopes k' and intercepts m' that were finally used to obtain the dynamic glucose concentration in sweat over the on-body test, using the following equations:

$$k' = f_{slope} g_{slope} k \quad (5)$$

$$m' = f_{intercept} g_{intercept} m \quad (6)$$

Notably, we selected to accomplish the off-body calibration of the sensors before the on-body tests to check its proper functioning. Indeed, the calibration graph was demonstrated to be maintained after the assessment of the on-body test, with a variation of less than the 3% of the slope and intercept (see Figure S9 in the Supporting Information as an example). Then, for the dynamic correction, the calculation of the f and g factors at every pH and T was performed by considering linearity between the two experimental factors that are the closest to the pH and T range measured in the corresponding on-body tests (i.e., assuming linearity between two close points and accomplishing extra or interpolation). For example, if the pH range is found to be 5.7−5.9 in the on-body test, we took the correction factors calculated at 5.5 and 6.6 for the slope and the intercept (Figure 4c) and interpolate the dynamic correction in the fitting line between these two points. Whether the T is measured to be in the range 32−34 °C, we took the correction factors calculated at 30 and 33 °C for the slope and the intercept (Figure 4d) and extrapolate the

https://dx.doi.org/10.1021/acs.analchem.0c02211
Anal. Chem. 2020, 92, 10153−10161

dynamic correction using the fitting line between these two points. In addition, for clarification, the reader can find the entire calculation process for one particular glucose concentration in the Supporting Information. The same calculations are applied to every single point of each dynamic on-body profile with the help of a mathematical code in Matlab.

In an ideal situation, it would be necessary to fit the data to a more complex algorithm that considers join influences of pH and T, to better cover the effect in the enzyme activity.[25,26] For this purpose, a bigger data bank comprising a larger number of experiments at different pH and T would be necessary. In addition, it would be important to include a correction based on the influence of the perspiration rate in the correction factors (by adding an extra sensor into the epidermal patch to quantify the sweat flow rate on the sensors' surface), while for resilience effect seems not necessary to be incorporated in the final correction (small changes in the calibration parameters were detected for drastic torsion deformations, exaggerating those movement occurring in the forehead of the athlete). Overall, the aim of the present work is to demonstrate that pH and T corrections are needed to approximate the results observed in on-body measurements to those obtained with the gold standard techniques.

Validation of the Glucose Biosensor Operating off- and on-Bodily. The developed epidermal patch for glucose detection was first validated under off-body operation, i.e., by collecting sweat samples and analyzing them with the epidermal patch operating by means of the peristaltic pump and with a gold standard technique (UV−vis[28] and/or IC,[9] as detailed in the Supporting Information). Notably, other authors have already reported on this approach for the glucose biosensors validation, but with the absence of pure on-body validation.[7] In a second step, the epidermal patch on-bodily operating in 9 tests was accomplished. The workout program in the bike (T1-T9) was as follows: (i) a 5 min warm up, (ii) 35 min low- to midintensity workup (65−75% of maximum heart rate), and (iii) a cool down step. The heartrate of the subject was monitored during the entire exercise program.

For the sweat collection, a modification of the regional absorbent patch method was used as reported elsewhere.[6] Briefly, an absorbent patch (absorbent material mounted in Hydrofilm tape) was placed on the forehead of the subject, while he/she was practicing exercise in a static bike, and was replaced every 10 min. Then, after detachment, the absorbent material was squeezed with a syringe into vial to extract the sample, which was briefly stored at 4 °C until analysis. More details about the sweat collection method are provided in the Supporting Information. Before starting the sport practice (time 0 min), because the subject was not sweating yet, iontophoresis was applied to the arm of the individual to collect sweat. Blood tests were accomplished at time 0 min and also during the sport practice without stopping the exercise.

Figure 5a displays the correlation between the values found for glucose content in 16 different samples (collected during T1−T4 based on subject 1 and 2) analyzed with the epidermal patch (glucose biosensor) operating off-site the body (using the peristaltic pump) and the UV−vis method. Rather good correlation was obtained, as pointed out by Pearson correlation coefficient of 0.90. Table S1 in the Supporting Information displays the obtained values for glucose concentration and the percent difference between both techniques, being on average lower than the 10% and therefore confirming the observed

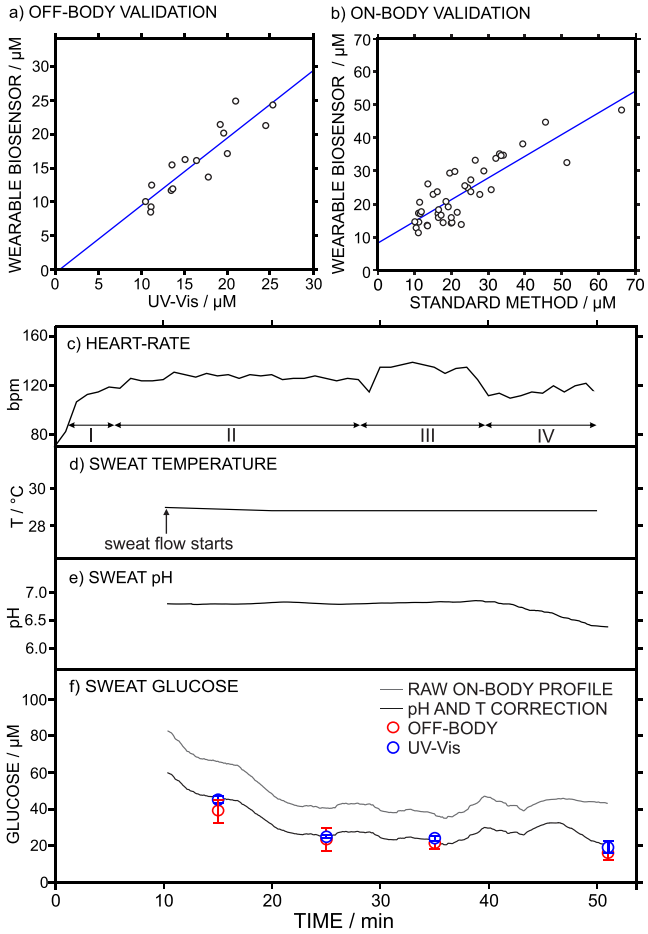

Figure 5. (a) Correlation in the off-body validation (n = 16). (b) Correlation in the on-body validation (n = 43). Profiles observed in the on-body test of subject 1 (T1): (c) Heart rate of the subject during the workout, which correlates the practice with the physical level (I, warm-up; II, low-intensity; III, midintensity; and IV, cool-down). (d) Sweat temperature. (e) Sweat pH. (f) Sweat glucose. Environmental conditions of 20 °C, relative humidity of 70%, 50 min cycling.

good correlation, while raw (not-corrected) data are further from the gold standard technique.

A total number of 9 on-body tests (T1-T9) were accomplished using the biosensor attached to the forehead of the subject together with the sampling pad. Before every test, all of the sensors were externally calibrated (see the Supporting Information). Figure 5b depicts the correlation of the glucose concentration found with the biosensor and the collected sweat samples analyzed by the gold standard technique (UV−vis or IC), corresponding this to the validation of real on-body measurements. Rather good correlation was obtained, as pointed out by Pearson correlation coefficient of 0.85 calculated for 43 samples (see Table S2 in the Supporting Information for the entire list of the raw data).

Studying now each on-body test (T1-T9) more in detail, Figure 5c depicts the heartrate monitored over T1, which may be used as a measure of the level of exercise, whereas Figure 5d−f shows the dynamic profiles for sweat temperature, pH, and glucose concentration, respectively. In addition, the glucose profile before and after the correction approach that considers dynamic pH and T fluctuations in sweat, together with sample analysis with UV−vis are provided in Figure 5f. As

https://dx.doi.org/10.1021/acs.analchem.0c02211
Anal. Chem. 2020, 92, 10153−10161

observed, the sweat temperature remained relatively constant over the entire on-body test (28.5 °C in average), whereas the pH experienced a decrease coinciding with the cool-dawn part of the workout (approximately from 6.8 to 6.4). Regarding the glucose profile, the concentration is higher at the beginning of the test (65 μM in average), followed by a decrease until a rather constant value after 20 min of the workout (25 μM in average), coinciding with the low/and mid/intensity activity, and further showing only minor fluctuations over the rest of the exercise. This trend is indeed expected, owing to the dilution of glucose in the eccrine glands of the skin while physical exercise continues.[16]

A comparison of the raw dynamic profile for glucose and that calculated after pH and T corrections with the measurements obtained with UV−vis (Figure 5f) revealed that, indeed, the corrected profile lies closer to the measurements provided by the standard method (less than 8% in percent difference, see Table S2 in the Supporting Information). Specifically, without pH and T correction, the percent difference with the standard technique range in the order of 20−30%. This trend was also observed for all of the 9 on-body tests accomplished in the present work even founding higher percentage differences (see Table S2 in the Supporting Information), therefore confirming the need for the developed "correction approach" for the response of the glucose biosensor. Any deviations from the values obtained with the gold standard technique may come from the further need of a joined pH−T correction together with any change in the perspiration rate, while contributing this latter in a lower extent to the final reliability of the outcomes (see above). Correction on the slope of the pH-selective electrode according to the T could be also considered toward an improved version of the presented correction, while adding complexity to the final algorithm.

Figure 6 presents the glucose dynamic profiles in sweat after pH and T correction that were observed in 8 different on-body tests (T2-T9) at different conditions. Figure 6a−c show the glucose profiles for the same subject at different times after food intake: 4, 3, and 1 h after lunch (T2-T4). A similar trend as that described in T1 was observed: initially, there is a higher glucose level, followed by a decrease during work-out, with the exception of the final point in T4, where an increase is observed during the cool down step. With no dependence on the time selected to assess the on-body test, the glucose level in the subject was always between 10 and 30 μM. Notably, on-body observations rather agree with UV−vis and the biosensor (in the epidermal patch) operating off-body, especially for longer workout times (see Table S1 in the Supporting Information).

Different glucose levels were found for each subject (Figures 5 and 6), and always within the expected physiological range:[21,22] subject 1 (T1) from 20 to 30 μM, subject 2 (T2-T4) from 10 to 30 μM, subject 3 (T5) from 10 to 25 μM, subject 4 (T6) from 10 to 20 μM, subject 5 (T7) constant level of approximately 30 μM, subject 6 (T8) constant level of approximately 20 μM, and subject 7 (T9) from 25 to 50 constant level of approximately 30 μM. Interestingly, all of the subjects follow the same trend of presenting a higher concentration at the start of the workout, followed by a stabilization at a lower glucose concentration. Regarding the intake of sugary drinks during the workout (Figure 6g,h), whereas subject 6 (T8) did not manifest a significant increase in glucose levels after the intake, subject 7 (T9) presented a gradual increase of almost double in the glucose concentration. Both subjects took 50 cL of the same commercially available isotonic drink. Some results previously pointed out that glucose taken during sport practice is quickly burnt, and therefore, it is not reflected in sweat glucose changes. Indeed, only a high consumption of sugar may lead to measurable changes in sweat glucose.[29] So far, our results likely reflect the different metabolism in each subject.

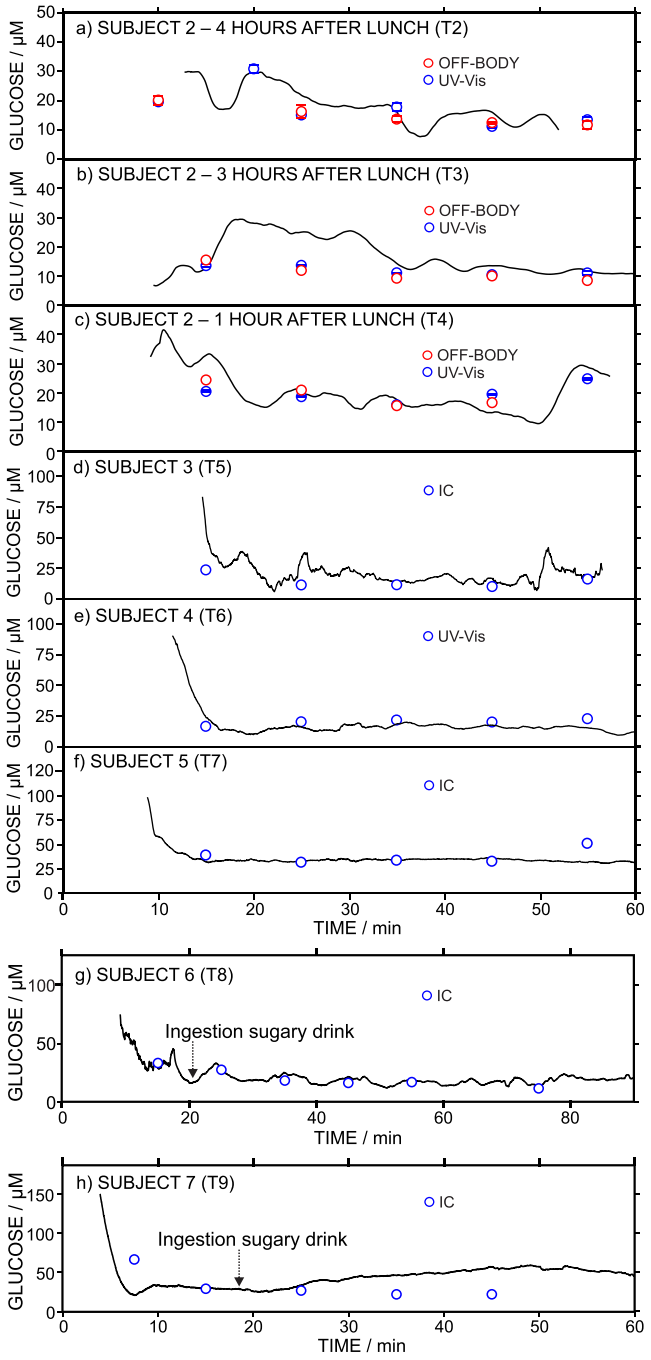

Figure 6. Dynamic glucose profiles observed during different on-body tests. Environmental conditions of 20 °C and relative humidity of 70%. Panels a−c correspond to the same subject practicing sport after different times of having lunch; panels d−f correspond to different subjects in the morning; and panels g and h correspond to other two subjects in the morning, with the difference that they took a sugary drink close to the 20 min of the sport practice.

https://dx.doi.org/10.1021/acs.analchem.0c02211
Anal. Chem. 2020, 92, 10153−10161

Variations found in pH and T between the different subjects as well as over the exercise practice of one subject rather justify the use of the developed correction approach. For example, in subjects 3−7 (Figure S11 in the Supporting Information), we found a pH range from 5.5 to 8.3 and a *T* range from 31 to 36 °C, with variations close to 0.8 pH units and 2 °C in the most extreme changes during the workout. Notably, it would be convenient to widen the calibration graph for pH up to 8.5 to encompas the entire pH range in further on-body experiments.

In particular, the highest deviation from the values obtained with the standard methods are observed in T9 from 30 min of the exercise (see Figure 6h), where both pH is low and the temperature high. Most likely, this points out the need for an algorithm contemplating the joint effect of pH and *T* for the correction of the biosensor response. Indeed, the consideration of the change in kinetics of both the enzyme[30] and the mediator[31,32] activity/behavior could be essential in such extreme case.

In all of the on-body tests, blood glucose was also analyzed at the beginning, middle, and end of the exercise time by means of a commercial glucometer (see the Supporting Information). In addition, glucose level in sweat before the workout was measured in sweat samples collected by iontophoresis using a commercially available device with clinical use approval.[33] The iontophoresis device was placed in the arm of the individual following the instructions of the manufacturer. Then, the sweat sample was introduced in the epidermal patch by means of the peristaltic pump and measure with the glucose biosensor.

Figure 7a displays the glucose values measured in each test, whereas Figure 7b presents the molar ratio between the glucose concentration in sweat and blood. Several trends are observed. First, the glucose amount in blood was always higher than in sweat, presenting molar ratios between 7 and 27 ($\times 10^3$) in the initial measurements. Subsequently, the same trend as for the sweat glucose in the on-body experiments was found: a decrease and a maintenance of the glucose concentration, somehow qualitatively confirming the outcomes of the wearable sensor during the 9 on-body tests.

However, no clear correlation was found between sweat and blood glucose concentration further than the same qualitative trend. When all the values were correlated (n = 26, Figure 7c), a Pearson coefficient of 0.55 was obtained, which does not confirm any clear correlation for the glucose measured in the two biological fluids. Indeed, if the correlation is restricted to only the initial measurements at t = 0 min (n = 7) or one subject (n = 5, T8), as shown in Figure 7d, the existence of a poor correlation was manifested with Person coefficients of 0.27 and 0.22, respectively. We are not the first to point out a poor correlation between glucose concentration in blood and sweat in individuals practicing sport.[7] On the other hand, there are some reports on existing glucose sweat and blood correlation (in absence of sport practice) claiming that any absence of correlation is due to improper sweat sampling.[34,35] Nevertheless, with the epidermal patch, no sampling is needed. Overall, massive studies are mandatory to clarify such correlation. Nevertheless, the main aim of the present work is not on the physiological side but the analytical development and evaluation of more reliable glucose measurements in sweat.

CONCLUSIONS

More reliable results are observed when the amperometric response of a wearable glucose biosensor is corrected by real-time fluctuations of pH and *T* in sweat during on-body measurements. Accordingly, a new epidermal patch containing a glucose biosensor as well as pH and *T* sensors implemented in a flexible microfluidic cell is herein proposed as a source for reliable physiological outcomes during sport practice. Our results are supported by a double validation accomplished with the sensing device operating off- and on-body. A number of 9 on-body tests involving different subjects under distinct conditions demonstrated rather good correlation with gold standard techniques. The developed methodology is expected to impact the design of the next generation of wearable chemical sensors, in particular those based on enzymatic sensors, aimed at more trustworthy data for sport and healthcare applications. To date, the success of wearable devices based on chemical sensors is based on the handling by the same researchers who invented the device. Importantly, pH and *T* correction will help these devices to work more independently while providing accurate outcomes.

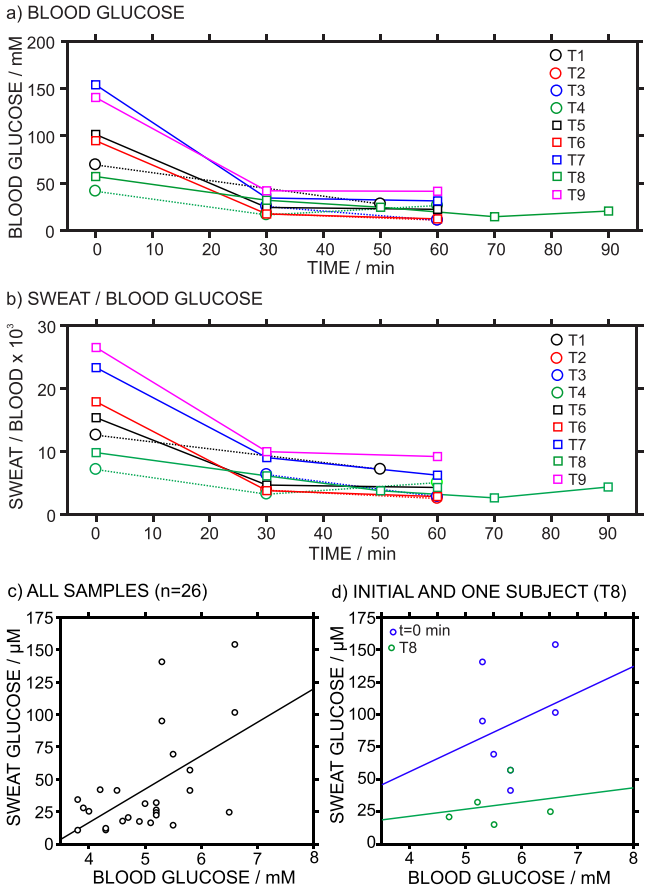

Figure 7. (a) Glucose concentration in blood measured with the glucometer at different times over the T1-T9. (b) Sweat/blood glucose concentration ratio observed at different times over T1-T9. (c) Correlation between blood and sweat concentrations (n = 26). (d) Correlation between blood and sweat concentrations observed at time 0 min for every subject (n = 6) and for only one subject over time (n = 5). Notably, the samples corresponding to time 0 min were collected by iontophoresis.

ASSOCIATED CONTENT

Supporting Information

The Supporting Information is available free of charge at https://pubs.acs.org/doi/10.1021/acs.analchem.0c02211.

https://dx.doi.org/10.1021/acs.analchem.0c02211
Anal. Chem. 2020, 92, 10153−10161

Details for the experimental section, raw data in on-body tests, and analytical characterization of the sensors (PDF)

AUTHOR INFORMATION

Corresponding Author

Gastón A. Crespo − *Department of Chemistry, School of Engineering Sciences in Chemistry, Biotechnology and Health, KTH Royal Institute of Technology, SE-100 44 Stockholm, Sweden;* orcid.org/0000-0002-1221-3906; Email: gacp@kth.se

Authors

Alexander Wiorek − *Department of Chemistry, School of Engineering Sciences in Chemistry, Biotechnology and Health, KTH Royal Institute of Technology, SE-100 44 Stockholm, Sweden*

Marc Parrilla − *Department of Chemistry, School of Engineering Sciences in Chemistry, Biotechnology and Health, KTH Royal Institute of Technology, SE-100 44 Stockholm, Sweden;* orcid.org/0000-0002-1344-8432

María Cuartero − *Department of Chemistry, School of Engineering Sciences in Chemistry, Biotechnology and Health, KTH Royal Institute of Technology, SE-100 44 Stockholm, Sweden;* orcid.org/0000-0002-3858-8466

Complete contact information is available at: https://pubs.acs.org/10.1021/acs.analchem.0c02211

Author Contributions

†A.W. and M.P. share first authorship.

Notes

The authors declare no competing financial interest.

ACKNOWLEDGMENTS

The authors acknowledge the financial support of KTH Royal Institute of Technology (Starting Grant, K-2017-0371) and the Swedish Research Council (VR-2017-4887). This project has received funding from the European Union's Horizon 2020 research and innovation programme under the Marie Skłodowska-Curie Grant Agreement No. 792824. We acknowledge the support of Mehdi Jalali, Kequan Xu, Renato Gil, and Rocio Canovas with the on-body tests.

REFERENCES

(1) Ray, T.; Choi, J.; Reeder, J.; Lee, S. P.; Aranyosi, A. J.; Ghaffari, R.; Rogers, J. A. *Curr. Opin. Biomed. Eng.* **2019**, *9*, 47−56.

(2) *Charter of Fundamental Rights (EU)*; 2000. DOI: 10.5040/9781849468350.ch-061

(3) Parrilla, M.; Cuartero, M.; Crespo, G. A. *TrAC, Trends Anal. Chem.* **2019**, *110*, 303−320.

(4) Bariya, M.; Nyein, H. Y. Y.; Javey, A. *Nat. Electron.* **2018**, *1* (3), 160−171.

(5) Hayward, J. *Wearable Technology Forecasts 2019−2029*; IDTechEx, 2019.

(6) Parrilla, M.; Ortiz-Gómez, I.; Canovas, R.; Salinas-Castillo, A.; Cuartero, M.; Crespo, G. A. *Anal. Chem.* **2019**, *91*, 8644−8651.

(7) Gao, W.; Emaminejad, S.; Nyein, H. Y. Y.; Challa, S.; Chen, K.; Peck, A.; Fahad, H. M.; Ota, H.; Shiraki, H.; Kiriya, D.; Lien, D.-H.; Brooks, G. A.; Davis, R. W.; Javey, A. *Nature* **2016**, *529* (7587), 509−514.

(8) Nyein, H. Y. Y.; Tai, L. C.; Ngo, Q. P.; Chao, M.; Zhang, G. B.; Gao, W.; Bariya, M.; Bullock, J.; Kim, H.; Fahad, H. M.; Javey, A. *ACS Sensors* **2018**, *3* (5), 944−952.

(9) Nyein, H. Y. Y.; Bariya, M.; Kivimäki, L.; Uusitalo, S.; Liaw, T. S.; Jansson, E.; Ahn, C. H.; Hangasky, J. A.; Zhao, J.; Lin, Y.; Happonen, T.; Chao, M.; Liedert, C.; Zhao, Y.; Tai, L.-C.; Hiltunen, J.; Javey, A. *Sci. Adv.* **2019**, *5* (8), No. eaaw9906.

(10) Cánovas, R.; Padrell Sánchez, S.; Parrilla, M.; Cuartero, M.; Crespo, G. A. *ACS Sensors* **2019**, *4* (9), 2524−2535.

(11) Kim, J.; Campbell, A. S.; Wang, J. *Talanta* **2018**, *177* (July), 163−170 2017.

(12) Kim, J.; Jeerapan, I.; Imani, S.; Cho, T. N.; Bandodkar, A.; Cinti, S.; Mercier, P. P.; Wang, J. *ACS Sensors* **2016**, *1* (8), 1011−1019.

(13) Van Enter, B. J.; Von Hauff, E. *Chem. Commun.* **2018**, *54* (40), 5032−5045.

(14) Lee, H.; Choi, T. K.; Lee, Y. B.; Cho, H. R.; Ghaffari, R.; Wang, L.; Choi, H. J.; Chung, T. D.; Lu, N.; Hyeon, T.; Choi, S. H.; Kim, D. H. *Nat. Nanotechnol.* **2016**, *11* (6), 566−572.

(15) Prieto, M. A.; Vazquez, J. A.; Murado, M. A. *Analyst* **2015**, *140*, 3587.

(16) Sonner, Z.; Wilder, E.; Heikenfeld, J.; Kasting, G.; Beyette, F.; Swaile, D.; Sherman, F.; Joyce, J.; Hagen, J.; Kelley-Loughnane, N.; Naik, R. *Biomicrofluidics* **2015**, *9* (3), 031301.

(17) Xu, X.; Karis, A. J.; Buller, M. J.; Santee, W. R. *Eur. J. Appl. Physiol.* **2013**, *113* (9), 2381−2389.

(18) Tse, J.; Rand, C.; Carroll, M.; Charnay, A.; Gordon, S.; Morales, B.; Vitez, S.; Le, M.; Weese-Mayer, D. *Acta Paediatr.* **2016**, *105* (3), No. e126.

(19) Romeijn, N.; Van Someren, E. J. W. *J. Biol. Rhythms* **2011**, *26* (1), 68−77.

(20) Smith, C. J.; Havenith, G. *Eur. J. Appl. Physiol.* **2011**, *111* (7), 1391−1404.

(21) Lee, H.; Hong, Y. J.; Baik, S.; Hyeon, T.; Kim, D. H. *Adv. Healthcare Mater.* **2018**, *7*, 1701150.

(22) Gao, W.; Brooks, G. A.; Klonoff, D. C. *J. Appl. Physiol.* **2018**, *124*, 548−556.

(23) Yokus, M. A.; Songkakul, T.; Pozdin, V. A.; Bozkurt, A.; Daniele, M. A. *Biosens. Bioelectron.* **2020**, *153*, 112038.

(24) Baker, L. B.; Ungaro, C. T.; Sopeña, B. C.; Nuccio, R. P.; Reimel, A. J.; Carter, J. M.; Stofan, J. R.; Barnes, K. A. *J. Appl. Physiol.* **2018**, *124*, 1304.

(25) Yetisen, A. K.; Martinez-Hurtado, J. L.; Ünal, B.; Khademhosseini, A.; Butt, H. *Adv. Mater.* **2018**, *30*, 1706910.

(26) Kong, D.; Le, L. T.; Li, Y.; Zunino, J. L.; Lee, W. *Langmuir* **2012**, *28* (37), 13467−13472.

(27) Issi, J. P.; Langer, L.; Heremans, J.; Olk, C. H. *Carbon* **1995**, *33* (7), 941−948.

(28) Perkampus, H.-H. *UV-VIS Spectroscopy and Its Applications*, 1st ed.; Springer-Verlag: Berlin, 1992.

(29) Coyle, E. F.; Coggan, A. R.; Hemmert, M. K.; Ivy, J. L. *J. Appl. Physiol.* **1986**, *61* (1), 165−172.

(30) González-Sáiz, J. M.; Pizarro, C. *Eur. Polym. J.* **2001**, *37* (3), 435−444.

(31) Araminaité, R.; Garjonyté, R.; Malinauskas, A. *Cent. Eur. J. Chem.* **2008**, *6* (2), 175−179.

(32) Pournaghi-Azar, M. H.; Ahour, F. *J. Solid State Electrochem.* **2010**, *14* (5), 823−828.

(33) https://www.elitechgroup.com/product/macroduct-sweat-collection-system-2.

(34) Moyer, J.; Wilson, D.; Finkelshtein, I.; Wong, B.; Potts, R. *Diabetes Technol. Ther.* **2012**, *14* (5), 398−402.

(35) La Count, T. D.; Jajack, A.; Heikenfeld, J.; Kasting, G. B. *J. Pharm. Sci.* **2019**, *108* (1), 364−371.